AWARD NUMBER: W81XWH-16-1-0067

TITLE: Define the Twist-ATX-LPAR1 Signaling Axis in Promoting Obesity-Associated Triple-Negative Breast Cancer

PRINCIPAL INVESTIGATOR: ANDREW MORRIS

CONTRACTING ORGANIZATION: University of Kentucky
Lexington, KY 40506-0509

REPORT DATE: AUGUST 2021

TYPE OF REPORT: FINAL

PREPARED FOR: U.S. Army Medical Research and Materiel Command
Fort Detrick, Maryland 21702-5012

DISTRIBUTION STATEMENT: Approved for Public Release; Distribution Unlimited

REPORT DOCUMENTATION PAGE

Form Approved

OMB No. 0704-0188

1. REPORT DATE
AUGUST 2021

2. REPORT TYPE:
FINAL

3. DATES COVERED
15APR2016 - 14APR2021

4.**TITLE AND SUBTITLE**

Define the Twist-ATX-LPAR1 Signaling Axis in Promoting Obesity-Associated Triple Negative Breast Cancer

4.CONTRACT NUMBER
W81XWH-16-1-0067

5b. GRANT NUMBER

5c. PROGRAM ELEMENT NUMBER

6. AUTHOR(S)

ANDREW MORRIS, Ph.D.

Professor, University of Kentucky College of Medicine

E-Mail: a.j.morris@uky.edu

5d. PROJECT NUMBER

5e. TASK NUMBER

5f. WORK UNIT NUMBER

7. PERFORMING ORGANIZATION NAME(S) AND ADDRESS(ES)

University of Kentucky

Lexington, KY 40506-0509

8. PERFORMING ORGANIZATION REPORT

9. CONTRACTING ORGANIZATION

U.S. Army Medical Research and Materiel Command
Fort Detrick, Maryland 21702-5012

10. SPONSOR/MONITOR'S ACRONYM(S)

11. SPONSOR/MONITOR'S REPORT NUMBER(S)

12. DISTRIBUTION / AVAILABILITY STATEMENT: Approved for Public Release; Distribution Unlimited

13. SUPPLEMENTARY NOTES

14. **ABSTRACT**

Breast cancer remains the second leading cause of cancer-related death in women worldwide. Triple negative breast cancer (TNBC) carries a poorer prognosis compared to other subtypes of breast cancer, given its higher genomic instability, tendency toward early metastasis, and lack of effective targeted therapies. As obesity is a risk factor for TNBC, understanding the mechanistic linkage between TNBC and obesity is crucial for the development of novel prevention and treatment strategies. TNBC activates the epithelial-mesenchymal transition (EMT) program mediated by EMT transcription factors, including Twist. Twist is highly expressed in TNBC cells, and its expression is positively correlated with metastatic potential. Our preliminary data showed that Twist interacted with BRD4 to regulate its target gene transcription, and Autotaxin (ATX) and LPAR1 were dramatically increased in Twist-overexpressing breast cancer cells and adipocytes. Encoded by the *ENPP2* gene, ATX is a secreted enzyme that produces most of the extracellular lysophosphatidic acid (LPA), which signals through its receptors (LPAR1-6) to mediate a wide range of inflammatory processes including wound healing, fibrosis and metastasis. Interestingly, both Twist and ATX were demonstrated to be involved in diet-induced obesity. Accordingly, we propose that Twist activation intensifies the ATX-LPAR1 signaling to promote the development and progression of obesity-associated TNBC.

15. SUBJECT TERMS

NONE LISTED

16. SECURITY CLASSIFICATION OF:			**17. LIMITATION OF ABSTRACT**	**18. NUMBER OF PAGES**	**19a. NAME OF RESPONSIBLE PERSON** USAMRMC
a. REPORT	**b. ABSTRACT**	**c. THIS PAGE**			
U	U	U	UU	17	**19b. TELEPHONE NUMBER** *(include area code)*

Standard Form 298 (Rev. 8-98)

Table of Contents

1. Introduction

Triple-negative breast cancer (TNBC) carries the poorest prognosis among breast cancer subtypes, given its high genomic instability, tendency toward early and recurrent metastases, and lack of effective targeted therapies. Standard surgery with adjuvant chemotherapy and radiotherapy offers limited efficacy once the tumor cells begin to metastasize. Epidemiological evidence strongly indicates the co-morbidity of TNBC and obesity; women with overweight/obesity are at a significantly higher risk of developing TNBC. The obesity rate has been increasing rapidly in the U.S. population over recent decades, posing another daunting threat to TNBC prevention and treatment. This study aims to elucidate the mechanistic linkage between TNBC and obesity for the development of novel targeted therapies. Specifically we found that a transcription factor called TWIST that is increased in both breast tumor cells and in breast adipose tissue increases the expression of genes encoding Autotaxin, an enzyme that generates a bioactive lipid called lysophosphatidic acid (LPA) and a particular LPA selective G protein coupled receptor LPAR1. This supports our hypothesis that Twist activation during inflammatory breast cancer development and progression exacerbates development of obesity associated TNBC. We propose studies to test this hypothesis using cell and animal models.

2. Keywords

ATX: Autotaxin

LPA: Lysophospahtidic acid

LPAR1: Lysophospahtidic acid receptor 1

TNBC: Triple negative breast cancer

RUNX1: Runt Related Transcription Factor 1

3. Accomplishments

3.1. Major goals and accomplishments

We hypothesize that Twist activation intensifies the inflammatory ATX-LPAR1 signaling to promote the development and progression of obesity-associated triple negative breast cancer (TNBC). The overall objective of this proposal is to delineate the function and regulation of Twist, and to explore the therapeutic potential of targeting Twist-ATX-LPAR1 axis in TNBC and obesity. Accordingly, we have defined three Major Tasks: 1 Characterize the function of Twist in regulating ATX and LPAR1 expression; 2 Delineate the role of Twist-ATX-LPAR1 axis during TNBC cell-adipocyte crosstalk; 3 Define the Twist-ATX-LPAR1 signaling axis in promoting obesity-associated TNBC *in vivo*.

Accomplishments related to Major Task 1, Subtask 1a: Determine whether Twist acetylation correlates with adipogenic differentiation (Dr. Lin)

We have successfully used an *in vitro* adipogenesis model as proposed. **Figure 1** shows the changes in adipocyte morphology before and after induction of differentiation. Quantification of triglyceride (TG) content is shown in **Figure 2**. Expression of adipogenesis markers Pref-1 (pre-adipocyte exclusive) and Fabp4 (surface marker of mature adipocyte) was quantified by RT-PCR (**Figure 3**).

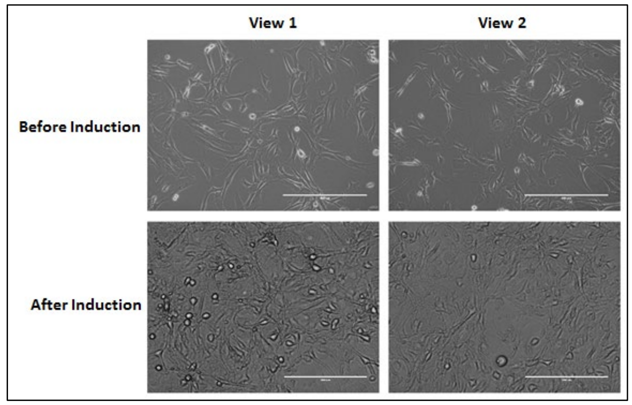

Figure 1 *In vitro* adipogenesis. Pre-adipocytes were induced according to adipogenesis protocol and images were taken under microscope.

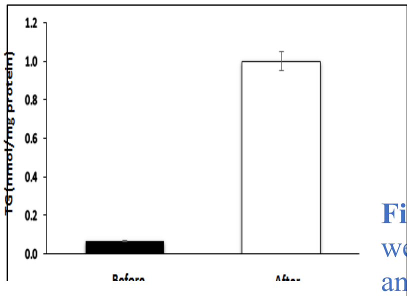

Figure 2 Quantification of TG content before and after induction of adipocyte differentiation.

After induction of adipogenic differentiation, samples were collected at different time points and Twist protein was enriched through immunoprecipitation. We found that Twist expression was dynamically regulated during adipogenesis, with its level reaching a peak at 48 hours post induction. In addition, Twist was significantly upregulated when cells were treated with interferons (**Figure 4**). At 48 hours after induction, Twist was immunoprecipitated and the level of di-acetylation was determined by Western blotting using a specific antibody developed by us (**Figure 5**). We found that diacetyl-twist was not detected in undifferentiated cells but the level of diacetyl-twist was increased in differentiated adipocytes, which is consistent with our hypothesis.

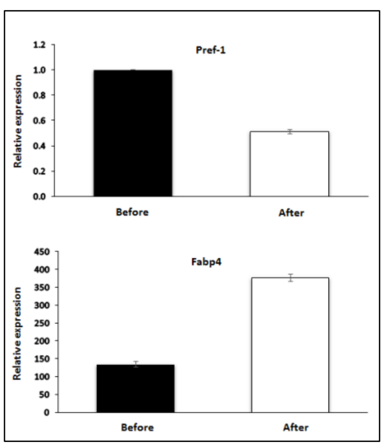

Figure 3 RT-PCR results indicate the relative mRNA levels of Pref-1 and Fabp4 before and after adipocyte differentiation. GAPDH was used as internal control.

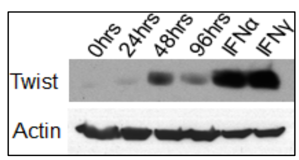

Figure 4 Pre-adipocytes were induced for differentiation and treated with interferons. Twist expression was examined at different time points

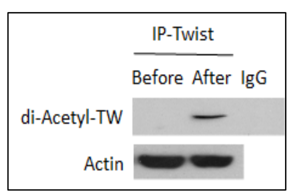

Figure 5 Before and after adipocyte differentiation, Twist was subject to IP and the level of di-acetylation was detected.

Accomplishments related to Major Task 1, Subtask 1b: Determine whether Twist activation regulates ATX synthesis and secretion by adipocytes/TNBC cells (Dr. Lin and Dr. Morris)

We have developed assays to measure ATX protein and activity *in vitro* that can be used to monitor ATX expression and activity in cells and tissues, as well as recombinant baculovirus vectors for expression of tagged forms of ATX that we can purify for use as controls for these studies. Some of these proteins contain His tags for purification and streptavidin binding peptide tag for detection (**Figure 6**).

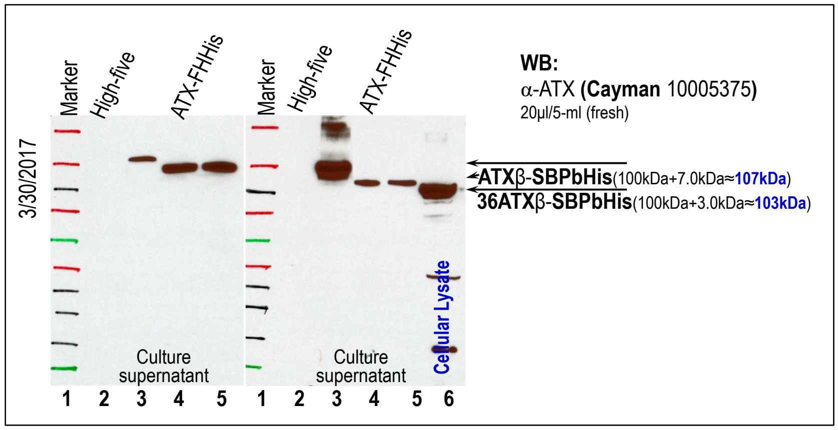

Figure 6 Expression of autotaxin in insect cells using baculovirus vectors. Cells were infected with recombinant baculoviruses for expression of the indicated autotaxin

In addition, we have applied CRISPR technology to examine if Twist enhances ATX and LPAR1 expression. Specifically we performed lentiviral transduction of Twist-targeting gRNA into breast cancer cells MDA-MB-578 and SUM-1315, and selected single cell colony with Twist knockout. We chose CRISPR-gRNA over the shRNA system which was originally proposed, as CRISPR provides higher specificity and fewer off-target effects. To verify knockout of Twist, we first performed mismatch cleavage assay using the KAPA HIFI hot start PCR kit and T7E1 enzyme from NEB. We designed two independent primer sets and performed PCR to detect single base mismatches or small insertions/deletions harbored in the selected single cell colonies. Gel electrophoresis showed cleaved products from Twist knockout cell samples compared to parental control, indicating the presence of heteroduplexes that can be recognized by T7E1 (**Figure 7**). Next, we performed Western blot to examine the expression of Twist as well as Vimentin, which is one of known Twist target genes. As expected, Twist expression was almost completely abolished, and Vimentin expression was significantly decreased in these selected single cell colonies (**Figure 8**). Furthermore, we performed RT-PCR and confirmed the downregulation of Wnt5a and DDR2, as well as upregulation of CDH1, all of which are already known Twist target genes (**Figure 9**). Interestingly, knockout of Twist significantly changed the morphology of MDA-MB-578 cells, as they notably lost branching compared to parental control (**Figure 10**). As knockout of Twist has been confirmed, we continued to examine the expression of ENPP2 and LPAR1 and found both proteins were partially downregulated (**Figure 11**).

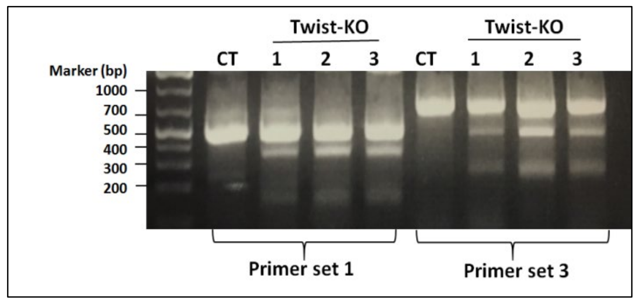

Figure 7 Mismatch cleavage assay showing introduction of single base mismatches or small insertions/deletions following lentiviral transduction of Twist gRNA into MDA-MB-578 cells

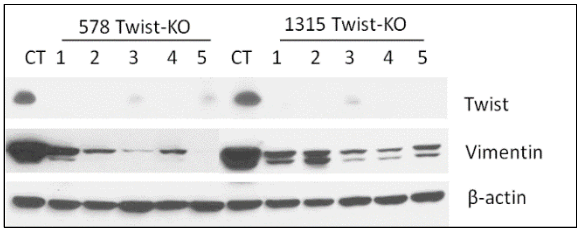

Figure 8 Western blot examining the expression of Twist and Vimentin in Twist knockout MDA-MB-578 and SUM-1315 cells

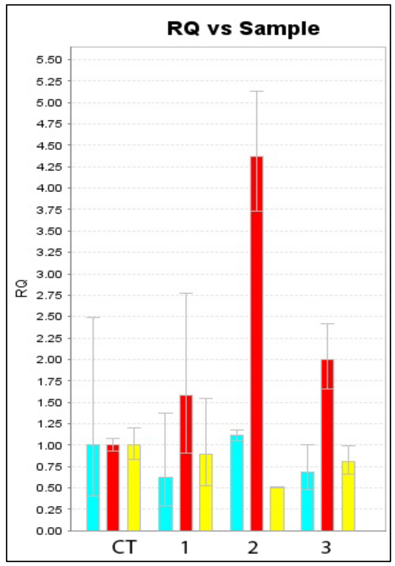

Figure 9 RT-PCR showing the expression of Wnt5a (blue), CDH1 (red) and DDR2 (yellow) in MDA-MB-578 clones (1-3) with knockout of

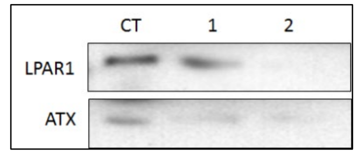

Figure 11 Western blot examining the expression of LPAR1 and ATX in MDA-MB-578 cells with Twist knockout (clones 1 and 2)

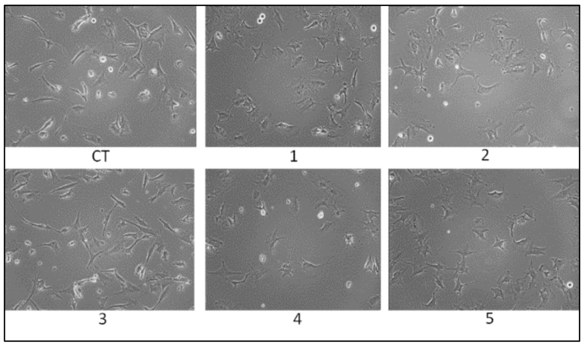

Figure 10 Morphology of MDA-MB-578 cells with knockout of Twist.

To further examine whether LPAR1 and ATX expression is regulated by Twist di-acetylation and its interaction with BRD4, we treated cells with TNF-alpha (to increase Twist di-acetylation) or the BET inhibitor JQ1 (to disrupt Twist-BRD4 interaction). We failed to detect significant change of expression of LPAR1 and ATX by Western blotting, due to limited sensitivity of commercial available antibodies. However, RT-PCR showed that TNF-alpha increased, while JQ1 decreased the expression of LPAR1 and ATX in adipocytes as well as breast cancer cells SUM1315 and Hs578T (**Figure 12**), which was consistent with our hypothesis. We plan to optimize the treatment conditions of JQ1 and TNF-alpha (drug concentration and duration of treatment) on adipocytes and various breast cancer cells (MDA-MB-231, SUM1315, BT549 and MDA-MB-157) in the future.

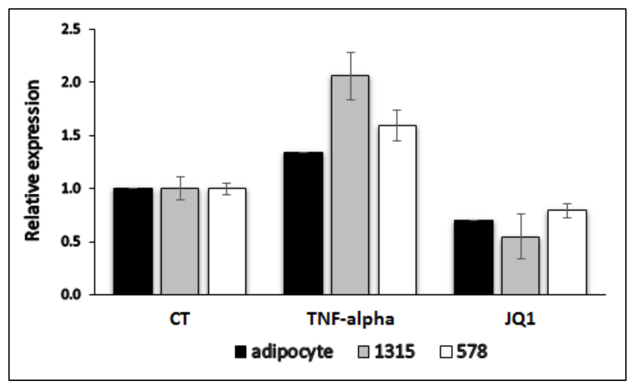

Figure 12 Human breast cancer cells and adipocytes were treated with TNF-alpha and JQ1, and the mRNA level of ENPP2 was examined by RT-PCR. GAPDH was used as internal control.

Accomplishments related to Major Task 1, Subtask 1c: Determine whether ENPP2 and LPAR1 are direct target genes of the Twist-BRD4 complex (Dr. Lin and Dr. Morris)

We performed analysis on the promoters of both genes and confirmed the presence of Twist-responsive E-boxes. We also refined the promoter regions to within 2000bp upstream of translation starting sites (**Figure 13**). Originally we planned to perform luciferase assay as well as ChIP assay to determine whether Twist directly regulates ENPP2 and LPAR1 expression. We successfully cloned the ENPP2 promoter and its proximal enhancer and generated a luciferase reporter construct (**Figure 14**). By performing dual-luciferase assay, we found that transfection of Twist only induced moderate change of luciferase activity (**Figure 15**), which was in contrast to our microarray data showing that Twist overexpression dramatically increased the mRNA level of ENPP2 and warranted further investigation (as shown in below sessions).

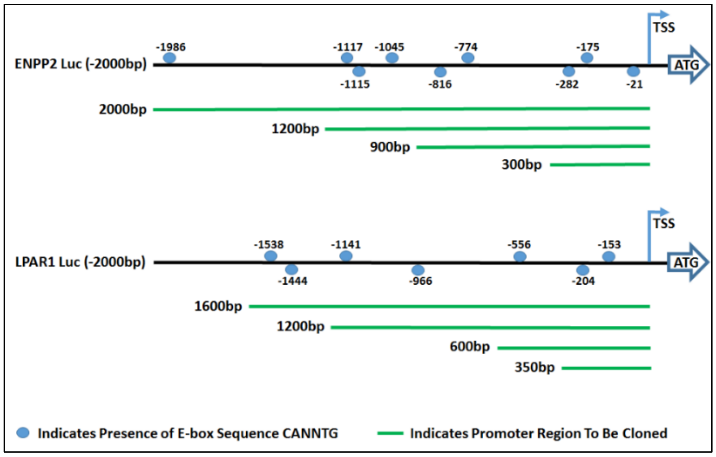

Figure 13 Graphic illustration of presence of E-box and sequence deletion promoter luciferase constructs.

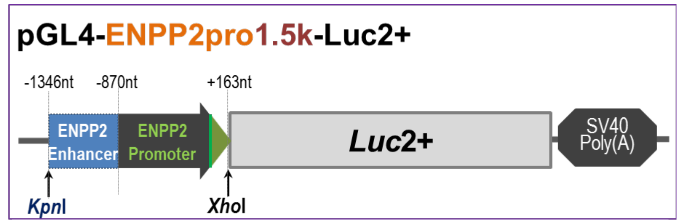

Figure 14 Schematic representation of ENPP2 promoter/enhancer luciferase construct.

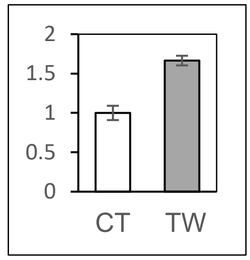

Figure 15 An ENPP2 promoter/enhancer luciferase construct was co-expressed with (TW) or without Twist (CT) in HEK293 cells. Cells were treated with 2mM TSA for 12 hours before luciferase

An alternative approach, as mentioned in the proposal, would be to perform human gene 2.0 ST array analyses in combination with deep sequencing (ChIP-Seq). This approach can determine direct targeting of ENPP2 and LPAR1 by Twist as well. In addition, we hypothesize that Twist can regulate the expression of other genes critical in the development of obesity-associated TNBC. The array-ChIP-Seq combination approach can provide comprehensive and unbiased data and better address this hypothesis. We have already completed the human gene 2.0 ST array analyses. We have also evaluated several commercial available Twist antibodies for ChIP-Seq.

Accomplishments related to Major Task 2, Subtask 2a: Determine the role of Twist-ATX-LPAR1 axis in modulating TNBC cell and adipocyte properties (Dr. Lin and Dr. Morris)

We have generated recombinant ATX for use in these studies. This includes a site directed mutant of ATX that lacks LPA generating enzymatic activity for use as a control in these studies. We have developed and refined mass spectrometry based methods to measure LPA and autotaxin substrates. These methods employ UPLC coupled electrospray ionization tandem mass spectrometry using a shimadzu UPLC system, a waters BEH C8 column and an ABSciex 6500 Q-trap mass spectrometer system operated in selected ion monitoring more (**Figure 16**).

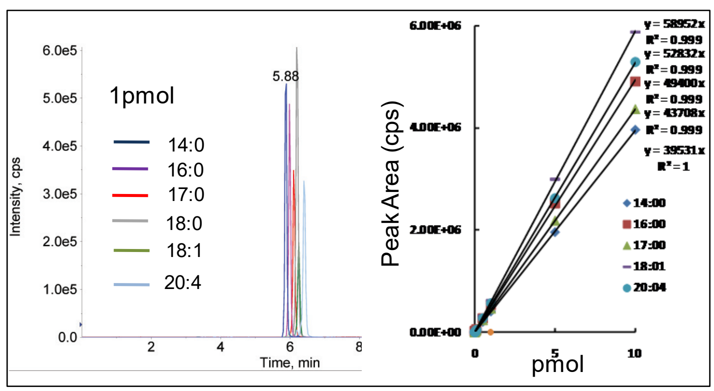

Figure 16 Measurement of Lysophosphatidic acid by tandem mass spectrometry. The indicated LPA species were separated and detected by mass spectrometry. The method is linear up to 10 pmol on the column with a limit of detection of ~10 fmol.

To determine whether the crosstalk between adipocytes and breast cancer cells is dependent on the Twist-ATX-LPAR1 axis, we performed adipocyte-breast cancer cell co-culture. In brief we cultured breast cancer cells in upper chamber and mouse 3T3-L1 in bottom chamber. JQ1, TNF-alpha or control solvent (DMSO) was added to the culture medium to regulate the expression of ATX and LPAR1. After co-culture, invasion assay was performed, as breast cancer cells passing through basement membrane layer and clinging to the bottom of the insert membrane were stained with crystal violet and quantified. All experiments were performed in triplicate. SUM1315 and Hs578T cells with Twist knockout were used as control. Since expression of ATX and LPAR1 is regulated by Twist, the Twist-ATX-LPAR1 axis is disrupted in these Twist knockout cells. As expected, TNF-alpha increased and JQ1 decreased the invasion of breast cancer cells, and knockout of Twist compromised the effect of TNF-alpha (**Figure 17**). We are also planning to use the co-culture system to test the effect of a highly specific ATX inhibitor PF8380 as well as LPAR1 antagonists on breast cancer cell invasion. In brief, experimental groups will be set up as (1) culture medium with LPA as positive control; (2) culture medium with ATX and its substrate (in order to generate LPA) as another positive control; (3) culture medium with only ATX substrates; and (4) culture medium with ATX substrates and ATX inhibitor/LPAR1 antagonist. We expect to find that addition of ATX inhibitor or LPAR1 antagonist will inhibit breast cancer cell invasion (experimental group (3) vs group (4)). Furthermore, we performed mammosphere formation assay using SUM1315 and Hs578T cells with or without Twist knockout. During culture, cells were treated with JQ1. Consistent with our hypothesis, JQ1 treatment or Twist knockout could inhibit mammosphere formation (**Figure 18**). Furthermore, we performed Western blotting to examine the expression of EMT markers and cancer stem cell (CSC) markers in the above-mentioned cells. As expected, we found that Twist knockout reduced the expression of CD44, Oct4 and Vimentin, and increased the expression of E-cadherin (**Figure 19**).

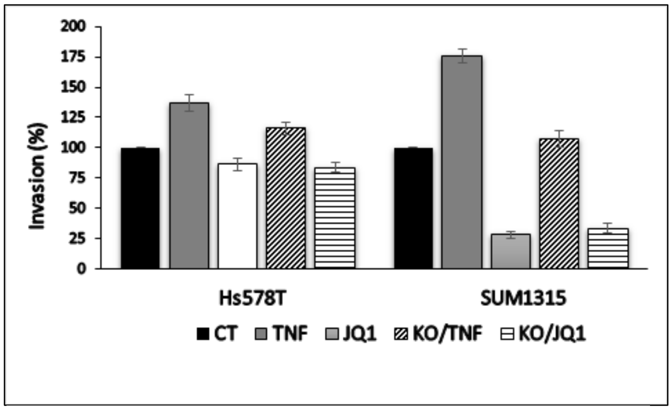

Figure 17 Hs578T and SUM1315 cells were treated with TNF-alpha and JQ1 and cell invasion assay was performed.

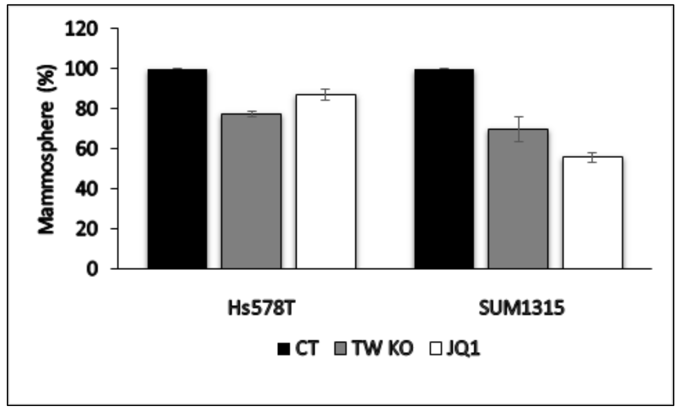

Figure 18 Hs578T and SUM1315 cells with or without Twist knockout were treated with JQ1 and mammosphere formation was examined.

It was found that breast cancer cells could induce delipidation (decrease of cellular TG content) of co-cultivated adipocytes. Adipocyte delipidation may happen to the tumor's benefit since it provides extra source of energy to fuel tumor growth and metastasis. To examine whether TNBC cell-conditioned media can cause delipidation of adipocytes, we performed TG quantification of 3T3-L1 adipocytes. Unexpectedly we only found modest changes of TG content in adipocytes cultured in conditioned media from TNBC cells with Twist knockout or JQ1 treatment compared to control (**Figure 20**).

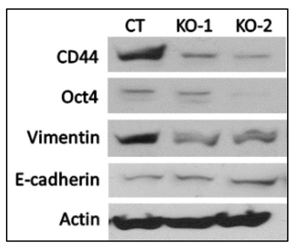

Figure 19 Western blot examining expression of EMT and CSC markers in SUM1315 cells with knockout of Twist.

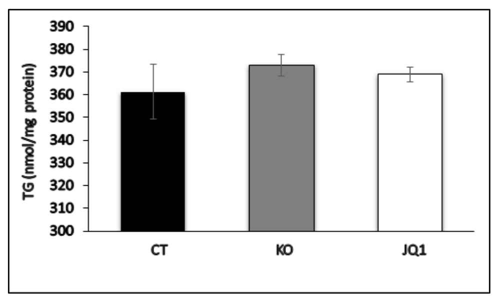

Figure 20 Cellular TG content was quantified in adipocytes cultured in TNBC cell-conditioned media.

In addition, we have generated recombinant ATX for use in these studies. This includes a site directed mutant of ATX that lacks LPA generating enzymatic activity for use as a control in these studies. We have developed and refined mass spectrometry based methods to measure LPA and autotaxin substrates. These methods employ UPLC coupled electrospray ionization tandem mass spectrometry using a shimadzu UPLC system, a waters BEH C8 column and an ABSciex 6500 Q-trap mass spectrometer system operated in selected ion

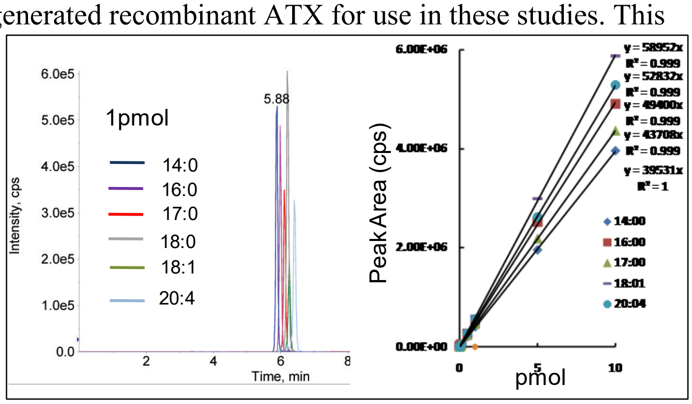

Figure 21 Measurement of Lysophosphatidic acid by tandem mass spectrometry. The indicated LPA species were separated and detected by mass spectrometry. The method is linear up to 10 pmol on the column with a limit of detection of ~10 fmol.

monitoring more (**Figure 21**). Taken together, we found that the Twist-ATX-LPAR1 axis is critical in mediating the crosstalk and properties of TNBC cells and adipocytes.

Accomplishments related to Major Task 2, Subtask 2b: Determine TNBC cell and adipocyte expression profiles mediated by Twist-ATX-LPAR1 signaling (Dr. Lin and Dr. Morris)

We originally planned to examine if blocking Twist-BRD4 with JQ1/MS417 could alter the TNBC cell expression profiles through human inflammatory cytokines & receptors PCR array as well as growth factors PCR array. In addition, we planned to examine human and mouse adipogenesis PCR arrays on adipocyte to profile the expression of 84 key genes involved in the differentiation and maintenance of mature adipocytes. These experiments were put on hold under the following considerations.

As we continued to characterize the transcriptional regulation of ENPP2, transfection of Twist only induced moderate change of luciferase expression driven by ENPP2 promoter (**Figures 14, 15**), which was in contrast to our microarray data showing that Twist overexpression dramatically increased the mRNA level of ENPP2. In addition, only modest changes of TG content in adipocytes cultured in conditioned media from TNBC cells with Twist knockout or JQ1 treatment was found (**Figure 20**). We performed RNA-Seq analysis of T47D-Twist stable cell line and confirmed the significant upregulation of ENPP2 mRNA upon Twist overexpression (**Figure 22**). To resolve the discrepancy, we decided to look further into transcriptional regulation of ENPP2. We hypothesized that there are additional layers of transcriptional regulation of ENPP2, as Twist may regulate ENPP2 expression indirectly by cooperating with other transcription factors or transactivate intermediate molecules to indirectly regulate ENPP2 transcription. Next, we searched the promoter/enhancer sequence of ENPP2 gene for binding motifs of other families of transcription factors. Indeed, we identified RUNX1 responsive elements, suggesting potential binding of RUNX1 (**Figure 23**). We then performed luciferase assay to find that co-transfection of Twist and RUNX1 further enhanced luciferase activity, in comparison to transcription in response to expression of either construct alone (**Figure 24**).

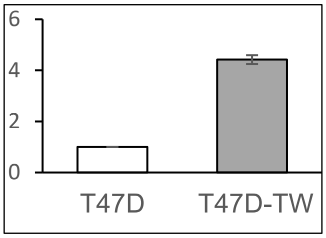

Figure 22 RNA-Seq showing that mRNA level of ENPP2 was significantly increased in T47D cells with Twist

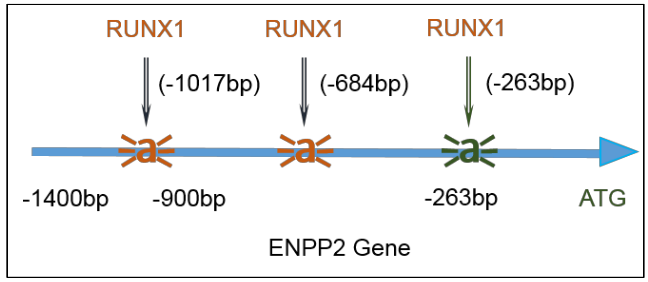

Figure 23 Schematic representation of potential RUNX1 binding sites on ENPP2 gene promoter and enhancer.

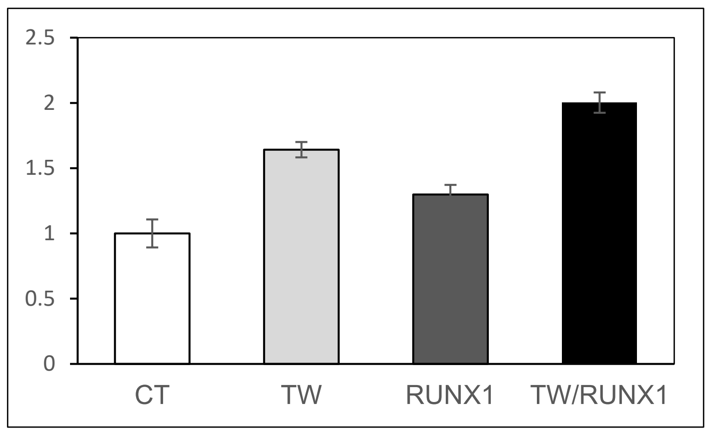

Figure 24 An ENPP2 promoter/enhancer luciferase construct was co-expressed with (1) Twist, (2) RUNX1 or (3) Twist and RUNX1 in HEK293 cells. Cells were treated with 2mM TSA for 12 hours before luciferase activities were measured.

Deregulation of RUNX1 has been associated with various malignancies, including breast cancer. Consistently, we found that RUNX1 is highly expressed in TNBC cell lines compared to luminal counterparts (**Figure 25**). Furthermore, we performed both exogenous and endogenous co-immunoprecipitation and found that Twist interacts with RUNX1 (**Figure 26**). It remains to be found whether and how Twist-RUNX1 interaction can affect their binding of ENPP2 promoter/enhancer. Together, these results indicate that RUNX1 may play a role in Twist-mediated ENPP2 transcription. This is an important finding and highly relevant to the major goal of the project, which is to target the Twist-ATX-LPAR1 axis for the treatment of obesity-associated TNBC, as co-targeting of RUNX1 may more efficiently disrupt the signaling cascade and result in better therapeutic outcomes. Accordingly, we planned to further investigate the mechanism underlying co-regulation of Twist and RUNX1 on target gene transcription in TNBC cells and adipocytes. Once the mechanism is elucidated, we will examine how targeting both molecules or blocking their linkage may affect the expression profiles of the cells through PCR arrays as originally proposed.

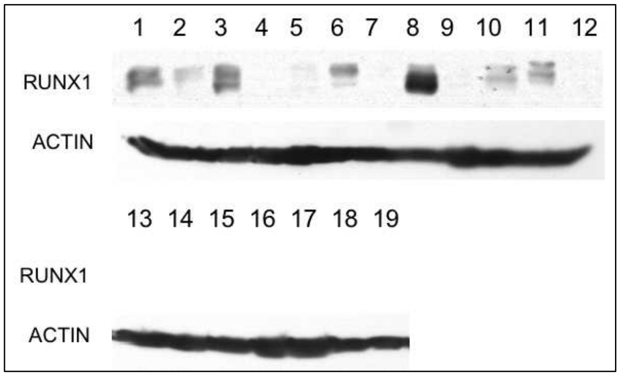

Figure 25 Western blot analysis of RUNX1 expression in multiple breast cancer cell lines. 1 MCF10A; 2 HMLE; 3 MDA-MB-231; 4 MDA-MB-157; 5 BT549; 6 Hs578T; 7 SUM1315; 8 SUM149; 9 SUM159; 10 MDA-MB-468; 11 BT20; 12 HCC1937; 13 MCF7; 14 T47D; 15 ZR75; 16 MDA-MB-361; 17 SKBR3; 18 BT483; 19 HCC1428

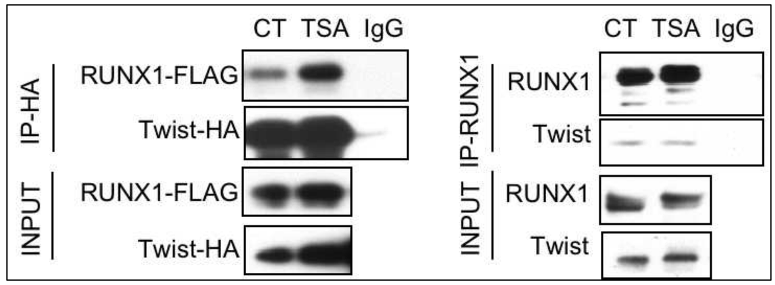

Figure 26 Left panel: HEK293 cells were co-transfected with Flag-tagged RUNX1 and HA-tagged Twist. Cells were treated with 2mM TSA or solvent control for 12 hours before being harvested. Twist protein was immunoprecipitated with HA and Flag-RUNX1 was examined by Western blot. Right panel: Hs578T cells were treated with TSA or solvent control as described above, and Twist-RUNX1 interaction was examined by co-immunoprecipitation followed by Western blot.

Accomplishments related to Major Task 3, Subtask 3a: Determine whether obesity facilitates the development of TNBC *in vivo* (Dr. Lin)

According to the original Statement of Work, mouse models will be used to test the *in vivo* function of the Twist-ATX-LPAR1 axis. Specifically, *BRCA1*$^{-/-}$ mice will be fed with high-fat diet and expression of Twist, ATX and LPAR1 will be examined. These animal experiments have been pending as we continue to collect and comprehensively analyze *in vitro* data about transcriptional regulation of ENPP2. We plan to start the *in vivo* experiment only for testing the mechanisms we verified *in vitro*. This is an ethical requirement for the use of animals in research. We also note that some of our key findings could not have been anticipated at the outset of the project. Consistent with good scientific practice we continue adjust our focus and research strategies based on the progress we have made, while ensuring that the work remains consistent with the major objective of the original proposal. In this case, elucidation of potential Twist-RUNX1 co-regulation on ENPP2 gene transcription through *in vitro* experiments will provide basis and rationale for relevant animal studies.

Accomplishments related to Major Task 3, Subtask 3b: Define the role of Twist-ATX-LPAR1 axis in tumorigenesis and metastasis of TNBC cells *in vivo* (Dr. Morris)

The broad goal of this task is to generate mice with adipocyte specific deficiency of ATX. These mice will then be used to determine the role of adipose derived ATX in breast cancer tumorigenesis and metastasis. Because we intend to explore the effect of diet induced obesity on breast cancer growth in these models we also examined the effect of feeding these mice an obesity promoting high fat diet. We have generated mice with adipocyte specific inactivation of the ENPP2 gene encoding ATX by crossing mice

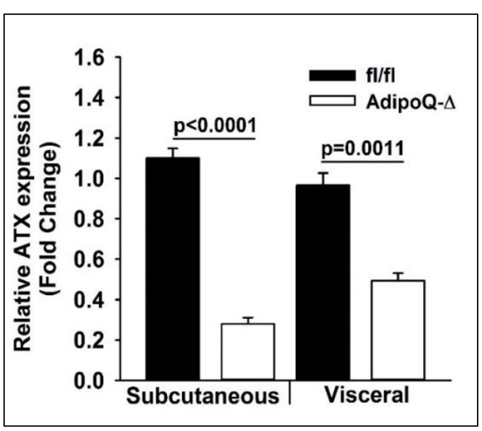

Figure 27 Adipocyte specific inactivation of ENPP2 encoding ATX in mice. ATX (ENPP2) mRNA levels were quantitated in visceral and subcutaneous adipose tissue from control (fl/lf) mice and the same strain expressing cre recombinase under control of the adiponectin promoter which is active after differentiation of fat cells. Mice harboring the cre deleted allele exhibited significant decreases in ATX (ENPP2) mRNA in subcutaneous and

expressing a cre recombinase transgene under control of the adiponectin promoter with mice carrying a "floxed" ENPP2 allele. These animals show significant systemic reductions in ATX levels in comparison to controls and these reductions are amplified in models of diet dependent obesity. **Figure 27** shows ATX mRNA levels in subcutaneous and visceral fat from control (fl/fl) mice and the same strain expressing cre recombinase under control of the adiponectin promoter.

In addition to adipocyte-specific knockout mice (Adipoq-Δ mice), we have also established a mouse model with systemic ATX reduction. Deletion of the *Enpp2* gene, encoding ATX, is embryonically lethal, therefore systemic ATX reduction was achieved postnatally by breeding mice with exons 3 and 4 of *Enpp2* flanked by lox-P sites (fl/fl) to mice carrying the Cre recombinase under the control of the MX-1 promoter and activating the promoter in neonatal pups with synthetic double-stranded RNA (MX1-Δ mice). To elicit diet-induced obesity, littermate mice with or without Cre recombinase were placed on HFD for 20 weeks. Global reduction in *Enpp2* expression was observed in MX1-Δ mice (open bars, **Figure 28A**), with significantly lower levels of gene expression in kidney and spleen, and to a lesser extent in heart and lung as compared to identically treated fl/fl littermate controls (dark bars; **Figure 28A**). ATX protein in subcutaneous and visceral adipose tissue was also lower in MX1-Δ as compared to fl/fl controls (**Figure 28B**). ATX activity was reduced by approximately 50% in plasma from MX1-Δ mice (**Figure 28C**). Together, these results confirm the effectiveness of the post-natal strategy to reduce *Enpp2* expression and ATX levels. No significant difference was observed between the MX1-Δ and fl/fl mice in weight gain on HFD (**Figure 28D**) or fat and lean mass after 20 weeks of diet (**Figure 28E**). No difference in heart, liver, lung or spleen weight was observed (data not shown). Interestingly, adipocyte cell size in both subcutaneous (**Figure 28F**) and visceral (**Figure 28G**) fat was significantly smaller in the MX1-Δ mice. In parallel with the changes in cell size, inflammatory marker expression in subcutaneous (**Figure 28H**) and visceral (**Figure 28I**) adipose tissue was also lower in MX1-Δ animals. In particular, gene expression for tumor necrosis factor alpha (*Tnfα,* interferon gamma (*Ifnγ,* interleukin-6 *(IL-6)* and chemokine CC motif ligand 2 (*Mcp1)* were all reduced in the MX1-Δ mice. These findings suggest a change in adipose response to diet-induced obesity in mice with reduced ATX levels.

We also examined the phenotype of Adipoq-Δ mice fed HFD for 20 weeks. No difference in kidney, spleen, lung, or heart *Enpp2* expression was observed between Adipoq-Δ mice and their fl/fl littermate controls (**Figure 29A**). ATX levels in subcutaneous fat were significantly reduced in Adipoq-Δ mice (**Figure 29B**), as was plasma ATX activity (**Figure 29C**). No difference in weight gain over 20 weeks on HFD diet was noted between the two groups (**Figure 29D**), and lean and fat body masses were similar (**Figure 29E**). Organs weights were also not different. As was observed with systemic ATX reduction, adipocyte-specific targeting of ATX resulted in smaller adipocyte size in mice fed HFD (**Figure 29F and 29G**), although not in mice on normal chow. Subcutaneous adipose (**Figure29H**) and visceral adipose (**Figure 29I**) from Adipoq-Δ mice also displayed lower levels of some but not all inflammatory cytokine gene expression. In particular, gene expression for *Tnfα*, *IL-6*, and *Mcp-1* were lower in Adipoq-Δ subcutaneous fat and for *Tnfα* and *Ifnγ* in Adipoq-Δ visceral fat (**Figure 29I**).

Accomplishments related to Major Task 3, Subtask 3c: Determine if Twist activation correlates with ATX and LPAR1 expression in TNBC specimens (Dr. Lin)

We evaluated Twist expression in 130 TNBC patients. Based on chi-square test performed by Dr. Chen, the biostatistician included in this project, there is no significant difference in the 5-year survival between patients with high vs. low expression of Twist. However, we did find that Twist expression in a different set of human primary TNBC specimens is positively correlated with tumor recurrence (**Figure 30**). We failed to generate ideal IHC results using our di-acetylated Twist antibody. This is possibly due to hindered/limited epitope recognition during tissue staining, as we do not have technical issues on performing IHC. Future research would include development of IHC-suitable di-acetylated Twist antibody, potential through contract with GenScript. Considering the role of RUNX1 in regulating ENPP2 transcription (**Figures 24-26**), we also plan to examine RUNX1 expression in TNBC samples following confirmatory *in vitro* experiments.

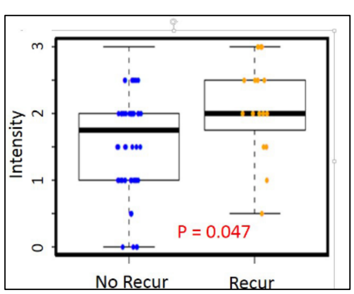

Figure 30 IHC was performed on Twist expression in 75 cases of TNBC samples with blinded scoring. Each tissue core was assigned an intensity score: negative (0), weak (1), moderate (2), and strong (3). Data were traced forward in time for 5 years to identify patients with recurrence. Box-and-whisker plot shows different expression levels. P-value was obtained from Wilcoxon signed-rank test.

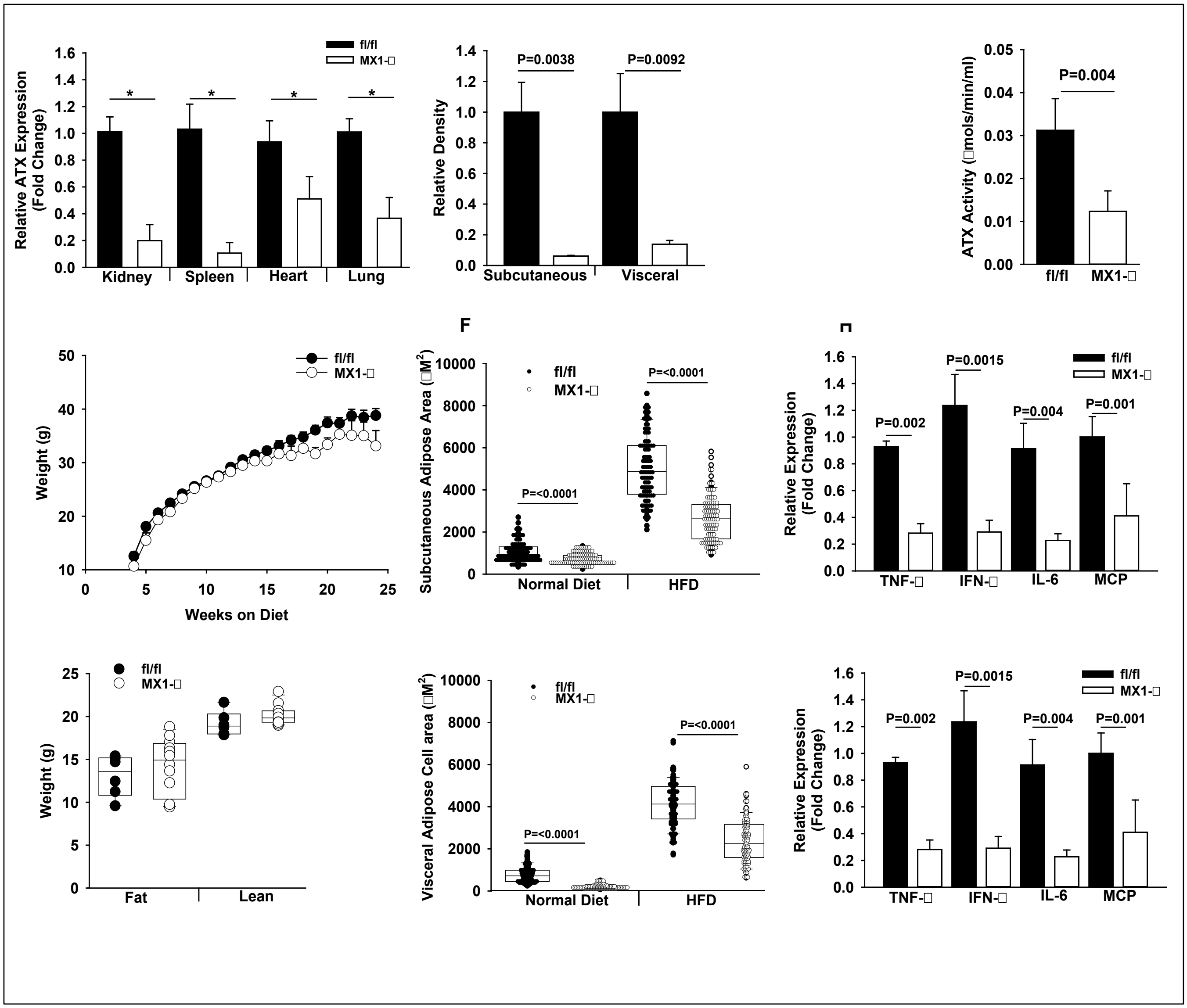

Figure 28 Characterization of mice with global post-natal reductions in ATX expression: Reduction in adipocyte size and adipose tissue inflammation without an effect on body weight after HFD. A.) Relative gene expression in different tissues in fl/fl (dark bars) and MX1-Δ (open bars) male mice (n=7). B.) ATX protein expression in subcutaneous and visceral fat. C.) Plasma ATX activity (μmols/min/ml) in fl/fl (dark bars) and MX1-Δ (open bars) male mice (n=7). D.) Average body weight in fl/fl (dark circles) and MX1-Δ (open bars) male mice (n=7) at the indicated times. Mice were placed on HFD at 4 weeks of age. E.) Body composition by fat and lean weight in fl/fl (dark circles) and MX1-Δ (open bars) male mice (n=5) after 20 weeks on HFD. F.) Cell area in subcutaneous adipose tissue in fl/fl (dark circles) and MX1-Δ (open bars) male mice (n=5) on normal chow or after 20 weeks on HFD. G.) Cell area in visceral adipose tissue in fl/fl (dark circles) and MX1-Δ (open bars) male mice (n=5) on normal chow or after 20 weeks on HFD. H.) Gene expression in subcutaneous adipose tissue from fl/fl (dark circles) and MX1-Δ (open bars) male mice after 20 weeks on HFD. I.) Inflammatory gene expression in visceral adipose tissue from fl/fl (dark circles) and MX1-Δ (open bars) male mice after 20 weeks on HFD. Comparison between genotypes was performed by t-test. * = P<0.05.

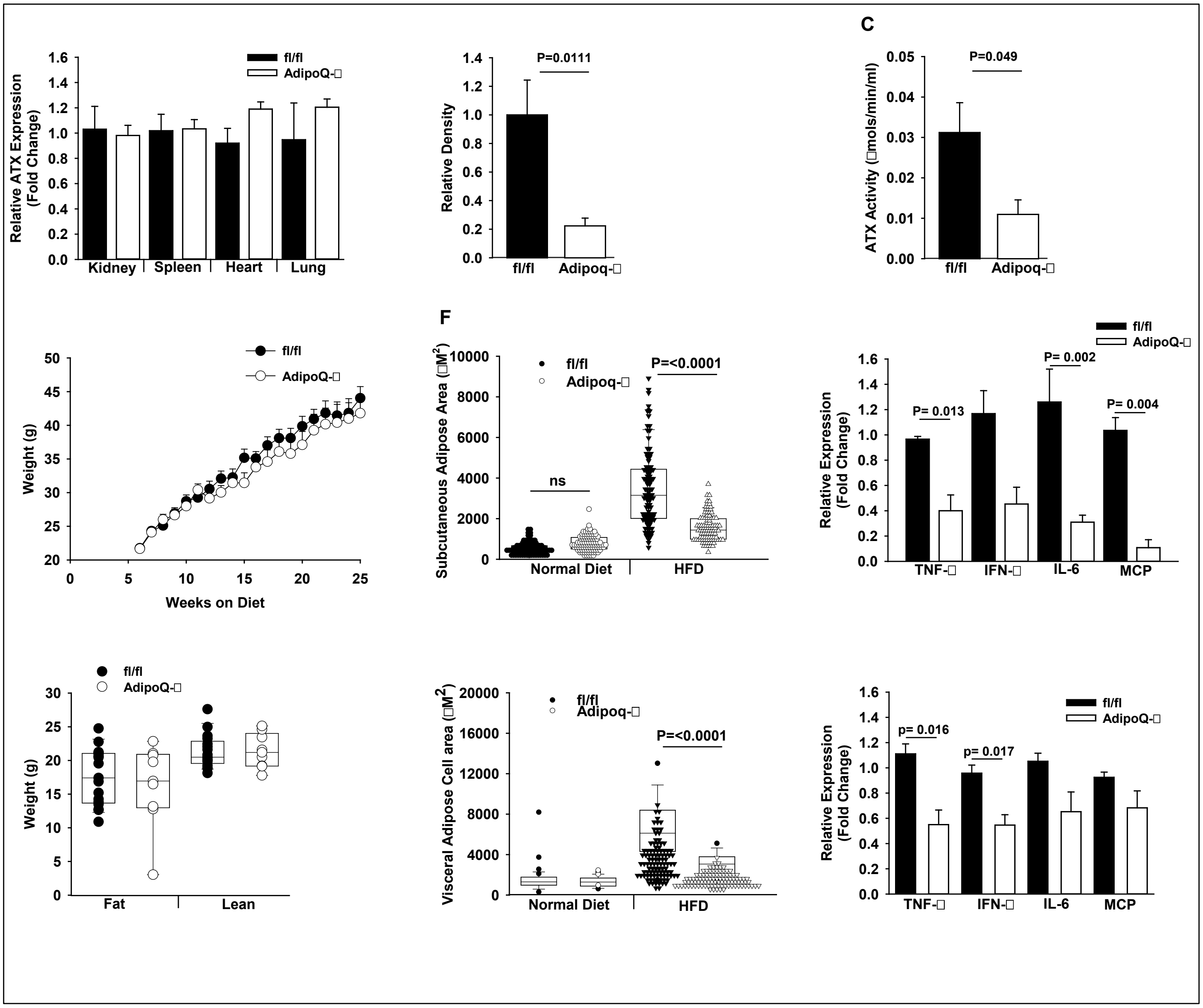

Figure 29 Characterization of mice with adipose specific reductions in ATX expression: Reduction in adipocyte size and adipose tissue inflammation without an effect on body weight after HFD. A.) Relative gene expression in different tissues in fl/fl (dark bars) and Adipoq-Δ (open bars) male mice (n=5). B.) ATX protein expression in subcutaneous and visceral fat. C.) Plasma ATX activity (µmols/min/ml) in fl/fl (dark bars) and Adipoq-Δ (open bars) male mice (n=5). D.) Average body weight in fl/fl (dark circles) and Adipoq-Δ (open bars) male mice (n=5) at the indicated times. Mice were placed on HFD at 4 weeks of age. E.) Body composition by fat and lean weight in fl/fl (dark circles) and Adipoq-Δ (open bars) male mice (n=5) after 20 weeks on HFD. F.) Cell area in subcutaneous adipose tissue in fl/fl (dark circles) and Adipoq-Δ (open bars) male mice (n=5) on normal chow or after 20 weeks on HFD. G.) Cell area in visceral adipose tissue in fl/fl (dark circles) and Adipoq-Δ (open bars) male mice (n=5) on normal chow or after 20 weeks on HFD. H.) Gene expression in subcutaneous adipose tissue from fl/fl (dark circles) and Adipoq-Δ (open bars) male mice after 20 weeks on HFD. I.) Inflammatory gene expression in visceral adipose tissue from fl/fl (dark circles) and Adipoq-Δ (open bars) male mice after 20 weeks on HFD. Comparison between genotypes was performed by t-test. * = P<0.05.

4. Impact.

The most important findings from this work are that, contrary to the initial hypothesis proposed in the original application TWIST is not a major regulator of ENPP2 gene expression. However we identified other regulatory elements in the ENPP2 promoter that could account for increases in ENPP2 expression in settings of inflammation including breast cancer and further work (promoter reporter studies and eventually gene editing studies) will be needed to validate these mechanisms. We also showed that adipose tissue is a significant site of ENPP2 expression in mice and that consequently inactivation of ENPP2 in adipose tissue phenocopies reductions in whole body ENPP2 expression. This suggests that adipose expansion would be associated with increased systemic levels of autotaxin which, as we proposed originally, could contribute to increased cancer risks and poorer prognosis observed clinically. Again, more studies will be needed to further examine these possibilities, for example by using the mouse models of ENPP2 deficiency we developed in experimental cancer models.

5. Changes/Problems. The major problem encountered with this partnered award was that the studies conducted by the partnering PI did not substantiate the premise that the TWIST transcription factor is an important regulator of ENPP2 expression. Accordingly, the partnering PI took the position that the experimental mouse cancer model studies proposed in the original application were unwarranted so he was unwilling to pursue these. In the absence of this avenue of research my laboratory undertook studies of ENPP2 gene expression using computational approaches and promoter/reporter constructs to search for alternative regulators of expression of the gene. My laboratory also conducted a broader characterization of the mouse models of ENPP2 deficiency described above including published studies and some currently unpublished work using mass spectrometry/lipidomics to look at the effects of ENPP2 deficiency on autotaxin substrates and products and a series of related bioactive lipid mediators.

6. Products

In addition to the biological reagents noted above and in the interim progress reports. We contributed data to the following publications.

1: Smyth SS, Kraemer M, Yang L, Van Hoose P, Morris AJ. Roles for lysophosphatidic acid signaling in vascular development and disease. Biochim Biophys Acta Mol Cell Biol Lipids. 2020 Aug;1865(8):158734. doi: 10.1016/j.bbalip.2020.158734. Epub 2020 May 3. PMID: 32376340.

2: Onono FO, Morris AJ. Phospholipase D and Choline Metabolism. Handb Exp Pharmacol. 2020;259:205-218. doi: 10.1007/164_2019_320. PMID: 32086667; PMCID: PMC7768751.

3: Kraemer MP, Mao G, Hammill C, Yan B, Li Y, Onono F, Smyth SS, Morris AJ. Effects of diet and hyperlipidemia on levels and distribution of circulating lysophosphatidic acid. J Lipid Res. 2019 Nov;60(11):1818-1828. doi: 10.1194/jlr.M093096. Epub 2019 Sep 4. PMID: 31484695; PMCID: PMC6824489.

4: Brandon JA, Kraemer M, Vandra J, Halder S, Ubele M, Morris AJ, Smyth SS. Adipose-derived autotaxin regulates inflammation and steatosis associated with diet-induced obesity. PLoS One. 2019 Feb 7;14(2):e0208099. doi: 10.1371/journal.pone.0208099. PMID: 30730895; PMCID: PMC6366870.

5: D'Souza K, Nzirorera C, Cowie AM, Varghese GP, Trivedi P, Eichmann TO, Biswas D, Touaibia M, Morris AJ, Aidinis V, Kane DA, Pulinilkunnil T, Kienesberger PC. Autotaxin-LPA signaling contributes to obesity-induced insulin resistance in muscle and impairs mitochondrial metabolism. J Lipid Res. 2018 Oct;59(10):1805-1817. doi: 10.1194/jlr.M082008. Epub 2018 Aug 2. PMID: 30072447; PMCID: PMC6168304.

7. Participants and Other Collaborating Organizations

Name	**Andrew Morris, Ph.D.**
Project Role	**PI**
Researcher Identifier	https://orcid.org/0000-0003-1910-4865
Nearest Person Month Worked	**5**
Contribution	**Oversight of research, lipid analysis, writing**
Funding Support	

Name	**Guogen Mao**
Project Role	**Research Associate**
Researcher Identifier	NA
Nearest Person Month Worked	**24**
Contribution	**Analysis of ENPP2 promoter, ENPP2 expression**
Funding Support	

Name	**Suchismita Halder, Ph.D.**
Project Role	**Postdoctoral**
Researcher Identifier	
Nearest Person Month Worked	**24**
Contribution	**Lipid analysis**
Funding Support	

Name	**Liping Yang.**
Project Role	**Research Associate**
Researcher Identifier	
Nearest Person Month Worked	**12**
Contribution	**Generation and characterization of mouse models**
Funding Support	

Name	**Maria Kraemer.**
Project Role	**Post Doctoral**
Researcher Identifier	
Nearest Person Month Worked	**6**
Contribution	**Measurements of autotaxin activity**
Funding Support	

8. Special Reporting Requirements

None

9. Appendices.

N/A